Proceedings World Geothermal Congress 2020+1
Reykjavik, Iceland, April - October 2021

An Integrated Modelling Study of Hellisheidi Geothermal Reservoir

Pedram Mahzari[1], Catalina Sanchez-Roa[1], Ashley Stanton-Yonge Sesnic[1], Giuseppe Saldi[1], Thomas Mitchell[1], Eric H. Oelkers[1], Vala Hjorleifsdottir[2], Sandra Osk Snaebjornsdottir[2], Thomas Ratouis[2], Alberto Striolo[3], Adrian P. Jones[1]

[1]Department of Earth Sciences, University College London, UK

[2]OR, Reykjavik Energy, Iceland

[3]Chemical Engineering, University College London, UK

p.mahzari@ucl.ac.uk

Keywords: Geothermal reservoir, modeling, tracer test, geo-mechanics, fracture network, stress-dependent permeability

ABSTRACT

Performance of geothermal reservoirs can be controlled by the hydrodynamic, thermal, mechanical, and chemical interactions taking place during heat extraction. Fracture network characterization can affect the life span of geothermal reservoirs and operational constraints. In SW-Iceland Hellisheidi geothermal reservoir, production and re-injection of geothermal aqueous phase can cause significant permeability variations due to local changes of effective stress. To assess the long-term performance of the reservoir, numerical modelling can be employed to investigate coupled impacts of these complex processes.

Using the information acquired from laboratory experiments, a field-scale model was constructed to take into account the hydro-thermo-mechanical processes. The flow paths were tuned using results of tracer tests performed at the site. For the characterizing the flow paths, the stress dependent fracture permeability was used. After calibrating the model with detailed structural mapping field data and laboratory measurements, the distributions of fracture permeability and porosity throughout the reservoir were mapped. The reservoir has two permeable layers separated with relatively lower fracture connectivity. Also, spatial distribution of fracture porosity can indicate the favorable conditions for mixing between injected and formation fluids. The outcome of this multi-scale study sheds light on the long-term performance of Hellisheidi geothermal reservoir, which would be utilized to guide further development of the region.

1. INTRODUCTION

The long-term performance of geothermal reservoirs depends primarily on the combined effects of hydrodynamic, thermal, geo-mechanical, and geochemical processes taking place during heat extraction (Ruhaak, et al., 2017). These processes may become important at different stages of the geothermal exploitation; for instance, geochemical interactions such as dissolution and precipitation would evolve over a long period of water reinjection and production. However, geo-mechanical processes such as stress-dependent fluid flow would be important from beginning of production and reinjection, which may induce tremors (Diehl, et al., 2017).

The fracture network can play an essential role in the long-term performance of geothermal reservoirs. Fracture networks and their connectivity have significant impact on heat extraction efficiency (Pandey, et al., 2018), development of the geothermal field (Qu, et al., 2017), long-injectivity (Doe, et al., 2014), geochemical reaction paths (Pandey, et al., 2018), and geo-mechanical stress distribution (Rutqvist, 2015). To identify effective flow paths, a series of tracer tests are usually performed, where a thermally stable tracer is injected into wellbores. The recovery of the tracer is measured in neighbouring producing wellbores to generate plots of tracer concentration against time. The tracer arrival time in producing wellbores and profiles of tracer concentrations can be useful tools to characterise the flow paths. Conventionally, equations governing hydrodynamic flow are used to describe the flow through fracture networks and matrix/fracture fluid exchange (Ratouis, et al., 2019). The usual practice for calibrating the geological model is that, the spatial distributions of fracture porosity and permeability are tuned to match the results of tracer tests using hydrodynamic modelling (Snæbjornsdottir, et al., 2018). Having calibrated the fluid paths, the geological model can be employed for assessing the reservoir performance for short and long-term scenarios.

Here in this study the performance of Hellisheidi geothermal reservoir in SW Iceland has been evaluated through coupled hydro-thermo-mechanical process models. Taking account of the available data, the results of a tracer test performed on Hellisheidi reservoir were used to calibrate the fluid paths. A new approach is taken in this study coupling a high resolution geological model to a stress-dependent permeability distribution to match tracer test profiles (despite the conventional methods using hydrodynamic equations only). The results of this study reveal the importance of process-based simulations of tracer tests and the coupled impact of hydro-thermo-mechanical processes on geothermal reservoir development.

2. GEOLOGICAL DESCRIPTION OF THE SUBSURFACE RESERVOIR

The Hellisheidi geothermal reservoir in southwest Iceland has been selected for this study. The distribution of wells in the study site are shown in Figure 1 along with some geological features of the Husmuli area. A tracer tests was performed in June 2013 by injecting 100 kg of tracer (1,3,6-NTS: naphthalene solfunates) dissolved in 4 m3 of water, into the HN17 reinjection well for ~two hours followed by injection of tracer-free geothermal fluid. A series of monitoring wells with the largest quantities of tracer recovered were HE31, HE48, and HE44, which are located northeast of HN17 injection well. The northeast direction of tracer recovery highlights the fact that the northeast trending faults are the major contributor to the flow in this system.

The concentration of tracer in the collected monitoring wells fluids was measured using high performance liquid chromatography with detection limit of 0.2 µG per kg of water (Kristjansson, et al., 2016). Figure 2 illustrates the temporal concentrations of tracer recorded over a period of 200 days. The tracer could be detected at HE-31 wellbore after 14 days of injection (Snæbjornsdottir, et al., 2018). Also, the breakthrough of tracer in well HE48 took place after 18 days (Snæbjornsdottir, et al., 2018). The general shape of tracer profiles provides insight into the number of fracture networks and probable flow paths.

Drone mapping performed in this study of the fault and dike exposures on the surface provide insight into the fracture network and dominant flow paths. Figure 3 shows the trends of the fracture network and dikes detected on the surface. The northeast direction of the fracture network identified on the surface mapping is well-matched with the tracer test results. Hence, surface exposure of the fracture network can be employed as an indicator of the subsurface flow paths. Figure 4 illustrates the likely flow paths of tracer propagation throughout the reservoir as inferred from the surface mapping of the fracture networks. Due to fast breakthrough of tracer in HE31 (i.e. after 14 days), it can be conceived that the injected tracer flows directly in a conductive fracture conduit towards HE31 and then, the tracer followed a direct path to HE48, and HE44. It should be noted that the wells are perforated at different depth (layers), which would affect the tracer flow. These observations with aid of surface mapping of the fracture networks can be used to construct the distribution of permeability, porosity, and fracture density throughout the sector. In the study area, the flow in the subsurface basaltic formations of the study area is dominantly contained a fracture network whereas, the rock matrices contain much of the geothermal fluid, such that this system resembles a dual porosity fractured model. The average porosity and permeability of the formation was obtained from well testing and laboratory experiments (Ayala, 2010) and (Nara, et al., 2011), as reported in Table 1. It should be noted that the distribution of permeability and porosity in different layers in the geological model were quantified using a history matching process to match the tracer tests and information in Table 1.

One important aspect fractured reservoirs is significant variations in fracture permeability and porosity due to changes in local effective stress. In the system considered in this study, as injection continues into the HN17 wellbore, the fracture permeability in vicinity of the wellbore would be enhanced due to injection pressure, whereas the permeability of producing wells would be reduced due to higher effective stress. To account for this geo-mechanical behaviour, the results of a set of laboratory experiments performed on basaltic rocks were used to model the variation of fracture permeability with respect to effective stress, as illustrated in Figure 5 (Nara, et al., 2011). In this set of measurements, three parallel fractures were created in a basaltic rock sample. As can be seen in Figure 5, the logarithm of fracture permeability exhibits a linear relationship with effective stress. Using data published on basaltic rocks and the Hellisheidi reservoir (Kristjansson, et al., 2016), the geological model was populated with the information for running the history matching.

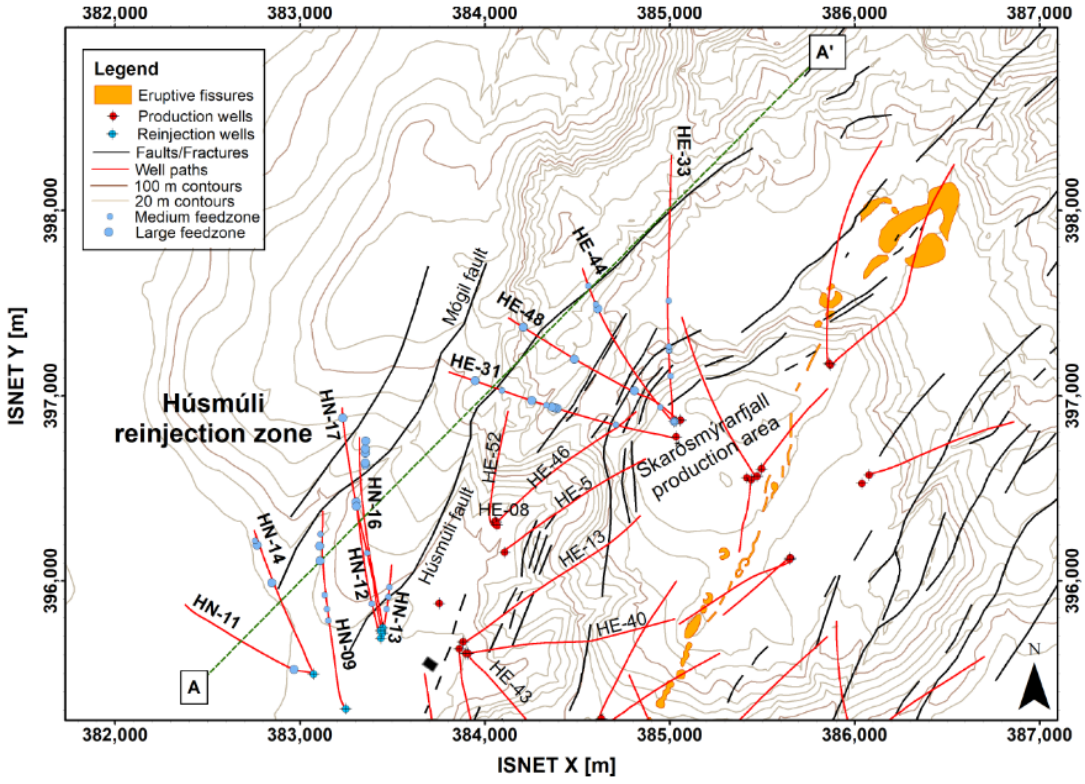

Figure 1: Hellisheidi geothermal reservoir considered for simulation study. HN17 well was used for batch tracer injection and wells HE31, HE48, HE44, HE33 showed the largest tracer recovery (Kristjansson, et al., 2016).

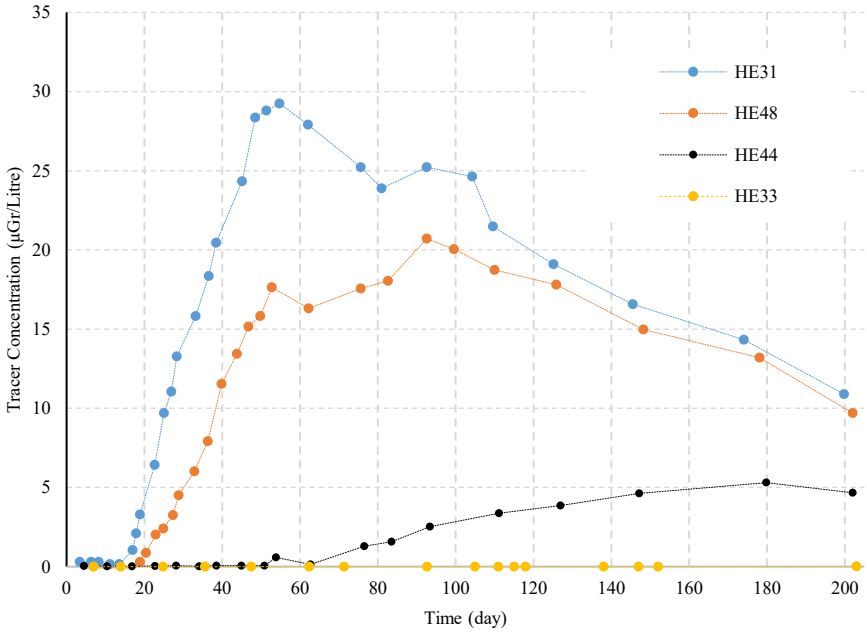

Figure 2: The temporal evolution of tracer (1,3,6 NTS) concentration as recovered in the producing wells (Kristjansson, et al., 2016).

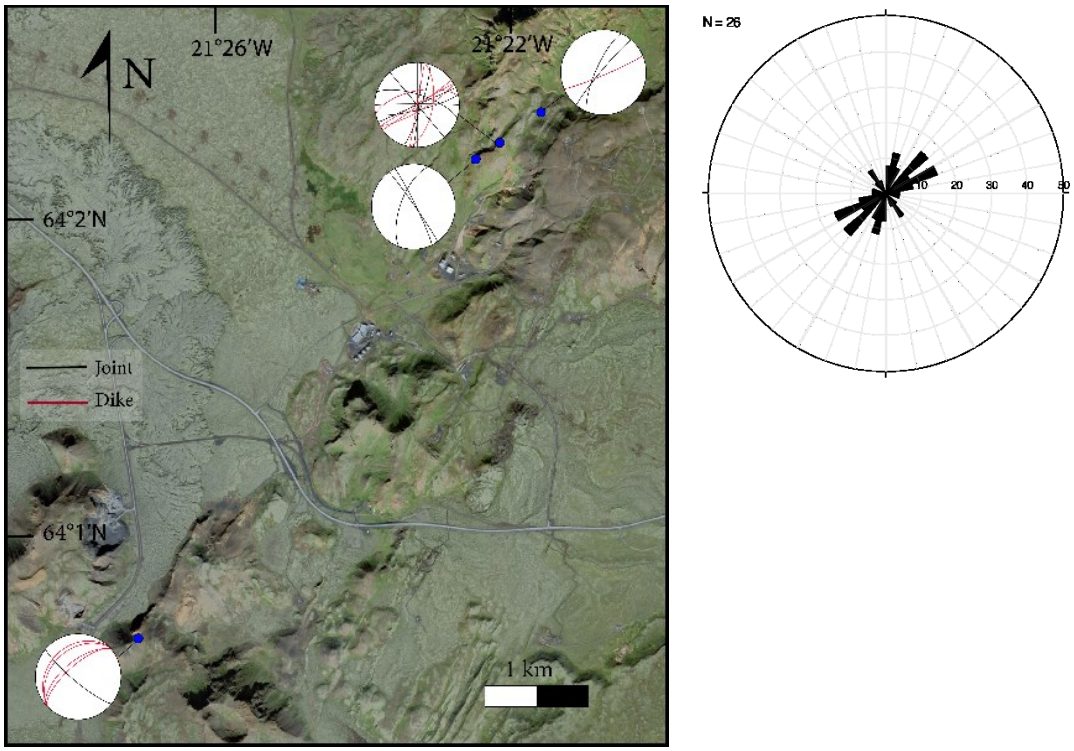

Figure 3: Direction of fracture and dikes in Hellisheidi region as identified from drone mapping. The dominant direction is southwest to northeast.

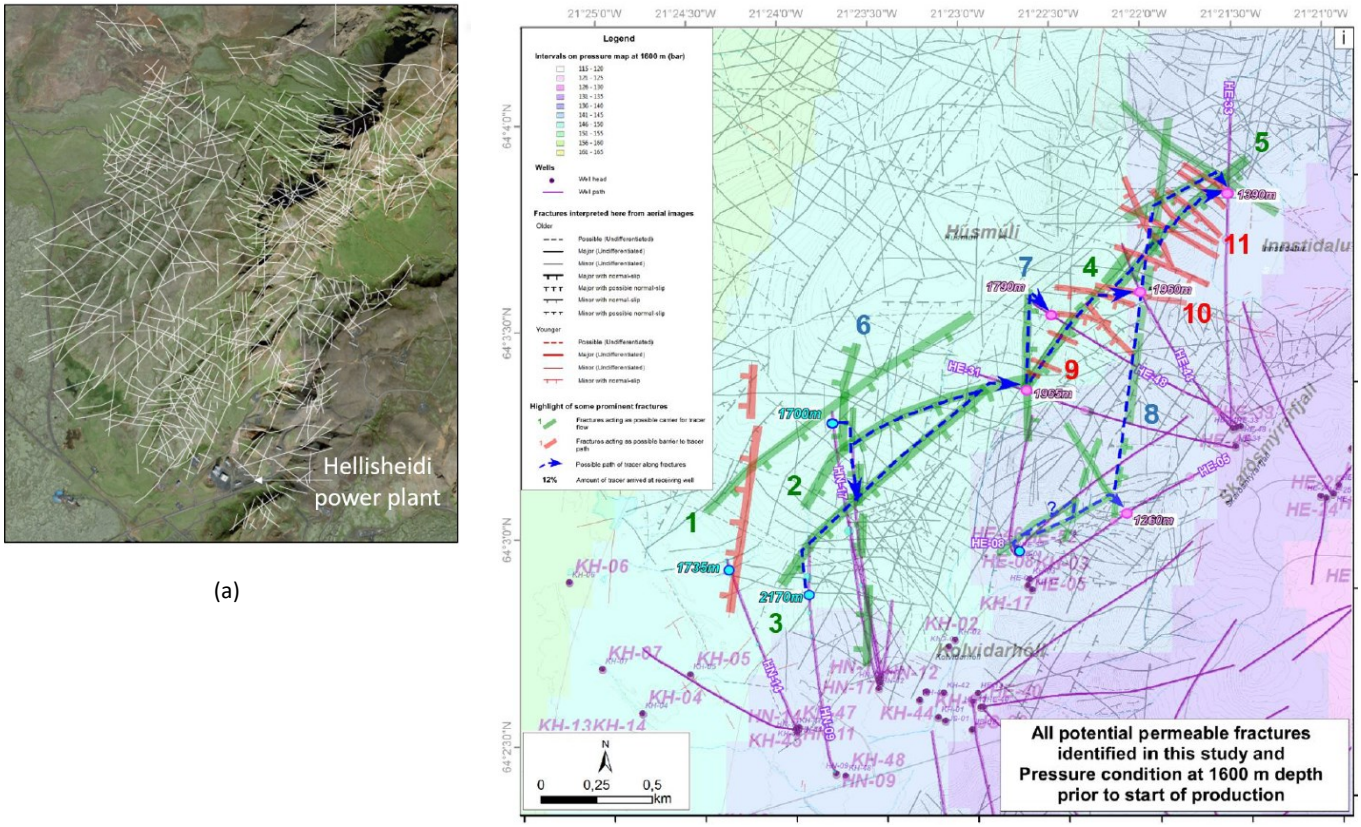

Figure 4: (a) The fracture network at the surface extracted from drone mapping images. (b) likely flow paths as inferred from the results of the tracer tests (Khodayar, et al., 2015).

Table 1: Inputs parameters used to construct the geological model for reservoir simulations.

Average fracture porosity (fraction)	0.01
Average horizontal fracture permeability (m^2)	87.5×10^{-15}
Average vertical fracture permeability (m^2)	8.75×10^{-15}
Fracture spacing (distance between fractures in metre)	50
Matrix porosity (fraction)	0.12
Matrix permeability (m^2)	0.1×10^{-15}

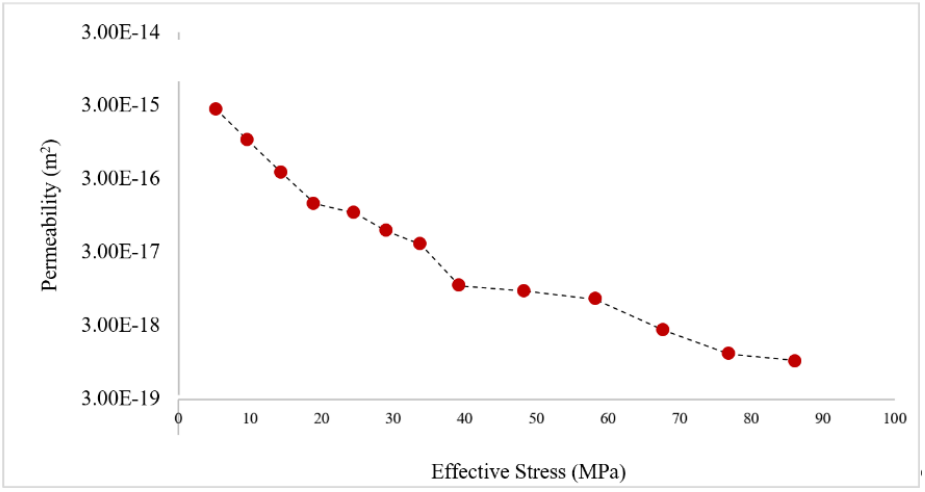

Figure 5: Laboratory measured stress-dependent fractrure permeability (three paallel fractures) of basaltic glass rock samples. Permeability is in logrithm scale.

3. MODELING APPROACH

A dual porosity for fractured flow was used to model the reservoir (Warren & Root, 1963). The distribution of fracture permeability and porosity, therefore would primarily control the flow. Hence, the fracture properties were tuned to match the tracer test profiles. Figure 6a illustrates the predominant faults in Hellisheidi reservoir, which were considered for constructing the permeability and porosity distributions, as depicted Figure 6b. The model has 7 layers with variable fracture permeability and porosity that can be adjusted to match the tracer results. For history matching, two multipliers were tuned for horizontal (longitudinal) and vertical (transverse) permeabilities. Also, additional multipliers were used for the three main flow paths as highlighted in Figure 6b. The flow paths and corresponding multipliers are considered for flow between HN17 and HE31 (but not for other producing wells). In total, 27 parameters (7 longitudinal permeability, 7 transverse permeability, 7 porosity multipliers, 6 additional multipliers for permeability and porosity of three paths) were used for the history matching process.

To optimise the objective function, the CMG DECE algorithm was used. It should be pointed out that CMG-GEM was used as the reservoir simulator. The geo-mechanical package (stress-dependent fracture permeability) of this software was used for history matching. The modelled fluid is a single-phase water. For history matching, the geochemistry package was not used since the effects of geochemical interactions on flow paths are likely to be insignificant for the 200 day period of the tracer test.

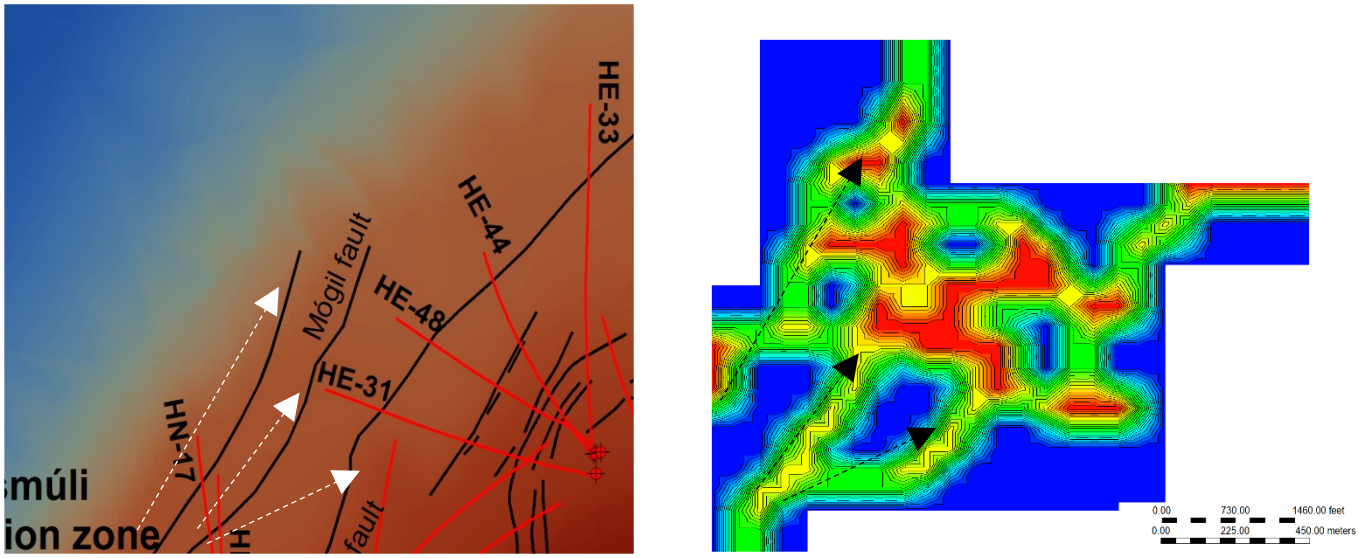

(a) (b)

Figure 6: (a) Schematic illustration of flow paths based on the inferred fracture network as shown in Figure 4. (b) fracture permeability distribution in the model to represent the three main flow paths. White arrows on (a) image highlight the three main flow path inferred from fault and dikes exposed in the surface mapping. However, black arrows on (b) is the three main fracture permeability flow paths constructed in the geological model.

4. HISTORY MATCHING RESULTS

Figure 7 depicts the results of history matching for the four producing wells. An acceptable similarity between the simulation results and field data was achieved. Not only the temporal profiles of tracer concentration were matched, the arrival time of the tracer in each producing was accurately reproduced. The success of the history matching suggests that the model is suitable for longer-term predictions. The 3D flow streamlines for the producing models have been generated using the calibrated model; the results are shown in Figure 8. From the streamlines, it can be inferred that the layers can communicate vertically. The streamlines of the HE31 well, which are depicted in red, an upward flow of the geothermal fluid is evident. On the other hand, the HE44 well (in yellow) is fed by the downward flow from the HN17 well top feedzone to the bottom of the feedzone of well HE44. Also, the HE48 (in yellow) producing well has a similar streamline pattern as well HE31. Figure 9 shows an aerial map of streamlines of the producing wells. The calibrated model indicates that the south-east part of the reservoir does not communicate with HE31 and the other production wells.

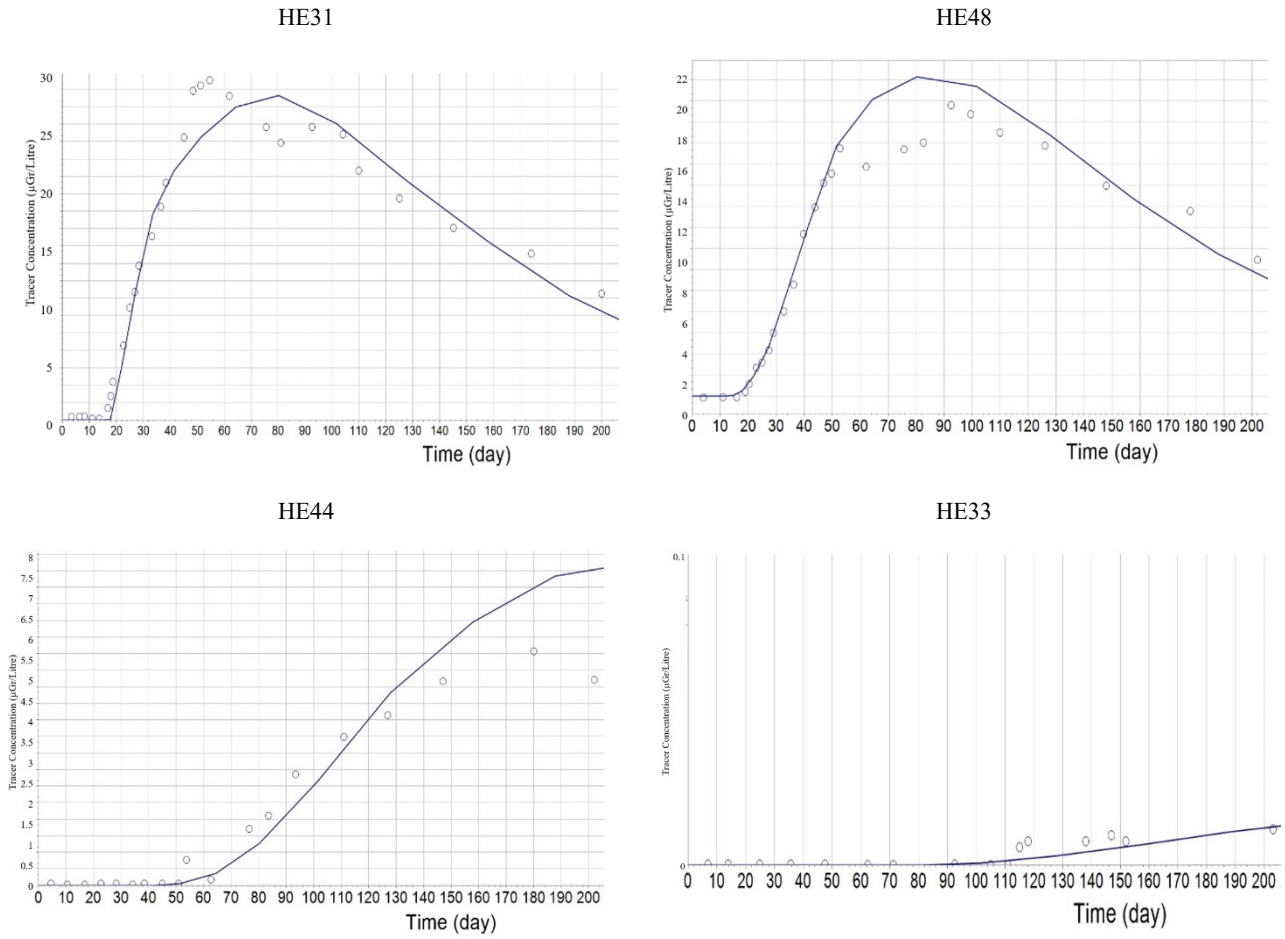

Figure 7: Results of history matching for the four producing wells showing tracer concentrations from field data (dots) and simulation results (continuous line).

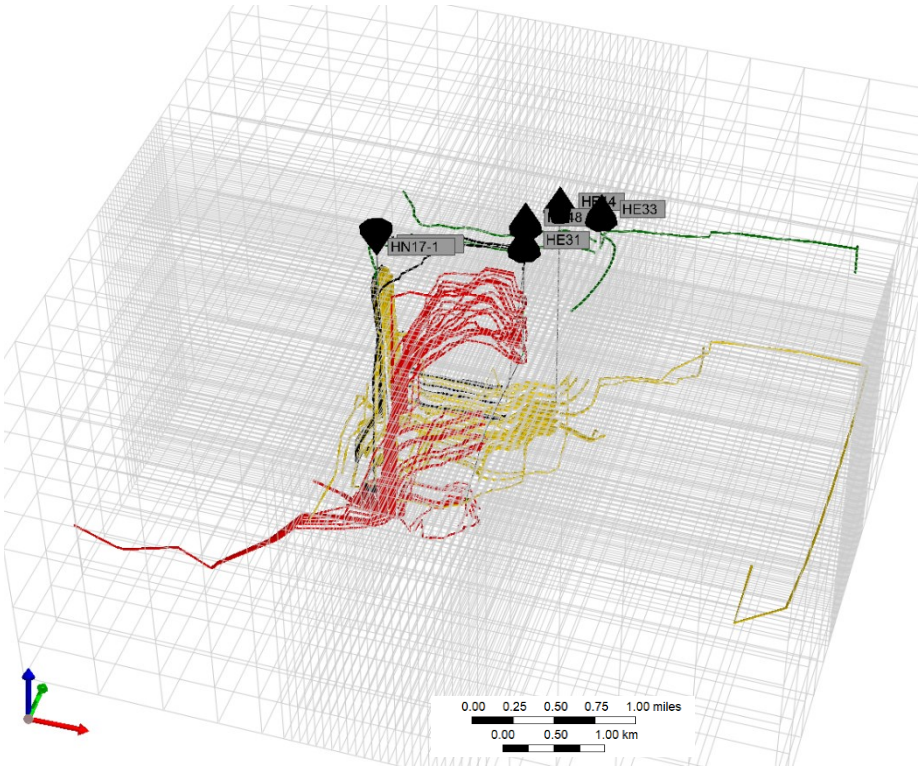

Figure 8: 3D streamlines of the fluid flow towards four producing wells. Red, yellow, black, and green streamlines represent flow towards wells HE31, HE48, HE44, and HE33, respectively. The downward and upward black cones represent the injection and producing wells, respectively.

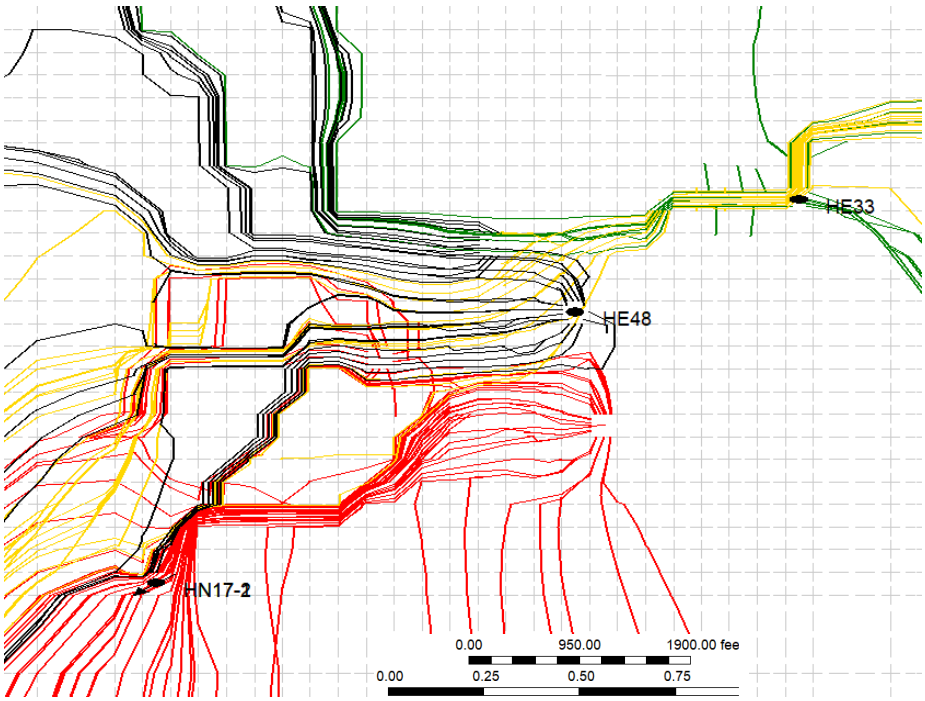

Figure 9: 2D streamlines of the flow to the four producing wells in layer 1 (top layer). Red, black, yellow, and green streamlines represent flow towards wells HE31, HE48, HE44, and HE33, respectively.

4.1 Vertical Distribution of Fracture Properties

Having matched the field data using the results of the tracer test, Figure 10 shows the multipliers for longitudinal (horizontal) fracture permeability for the various layers. This parameter determines the relative speed of the tracer travelling towards producing wells. Fracture permeabilities for different layers vary notably. As can be seem in this figure, fracture permeabilities for two layers are noticeably higher: layer 1 (top) and layer 5. These two layers are two feedzones perforated by the injection well. Figure 11 illustrates the multipliers for vertical fracture permeabilities tuned for the layers. This parameter indicates the communications between the layers. The layers next to the main injection feedzones have high vertical fracture permeabilities that allow the injected tracer to flow across the layers.

Figure 12 illustrates the fracture porosity tuned for each reservoir layer. Based on the history matching results, the reservoir has two distinct compartments. The top of the reservoir has a higher fracture porosity compared to the bottom. This feature in fracture porosity can be used as a helpful indication for further development of the reservoir for target perforations. The higher fracture porosity could provoke greater mixing between injection and formation fluids, which can lead to higher resident time for the injection fluid to interact with the formation rock and fluids.

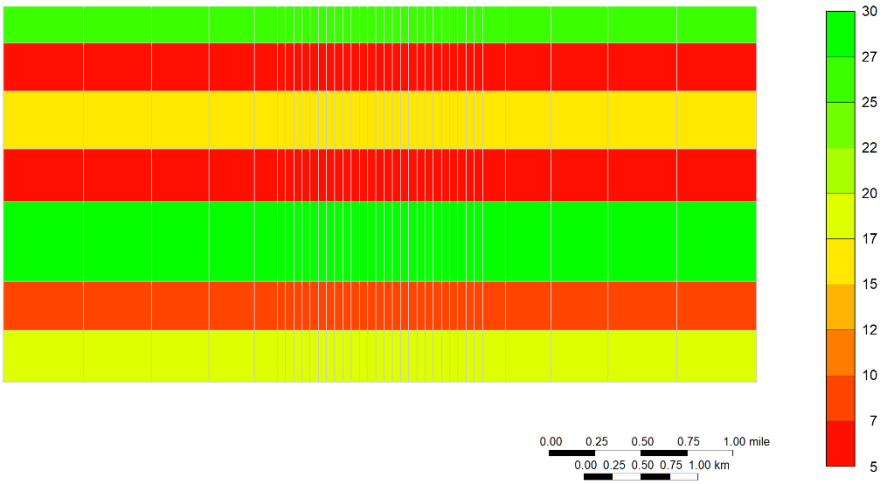

Figure 10: Multiplier for horizontal (longitudinal) fracture permeability as obtained from history matching.

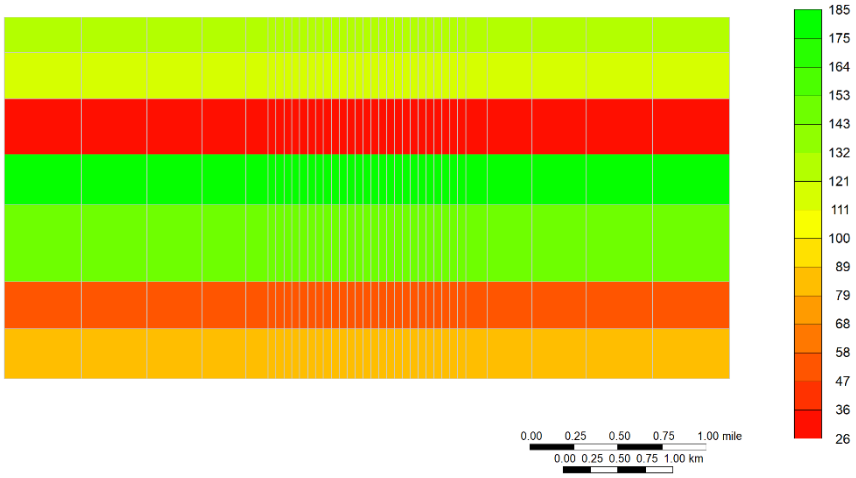

Figure 11: Multiplier for vertical (transverse) fracture permeability as obtained from history matching.

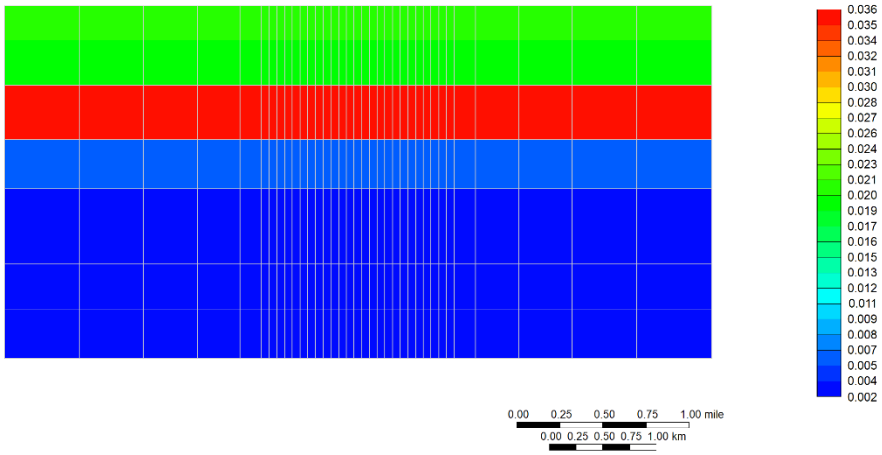

Figure 12: Tuned fracture porosity as obtained from history matching.

4.2 Spatial Distribution of Fracture Properties

Three main flow paths were identified based on geological observations and the temporal tracer profiles. The relative contributions of the flow paths needed to be adjusted to match the tracer profiles. The fracture porosity and permeability for these flow paths were tuned in addition to the properties of the seven layers. For the spatial distribution of the fracture porosity, five different regions were considered; three main flow paths between the injection well and HE31, the area between HE31 and HE48, and the area between HE48 and HE44. However, for spatial fracture permeability distribution, three main flow paths between the injection well and well HE31 were adjusted.

Figure 13 and Figure 14 illustrate the spatial distributions of fracture porosity and fracture permeability, respectively, as optimized by history matching of the tracer test results. The outcome of history matching indicates that the southern fracture path has higher porosity and lower permeability whereas, the northern flow path consists of a low porosity and high permeability fracture network. The understanding of the distribution of fracture permeability and porosity would be very helpful in the further management of the geothermal field. Based on the calibrated model, two faults (Mogil faults in Figure 6a) would have favourable fracture permeability contributing to the flow of geothermal fluid. Therefore, given the results of areal and vertical fracture distribution, the two Mogil faults intercepting the fourth layer (from top) can be considered as the sweet spot for sustainable flow and hence, heat extraction.

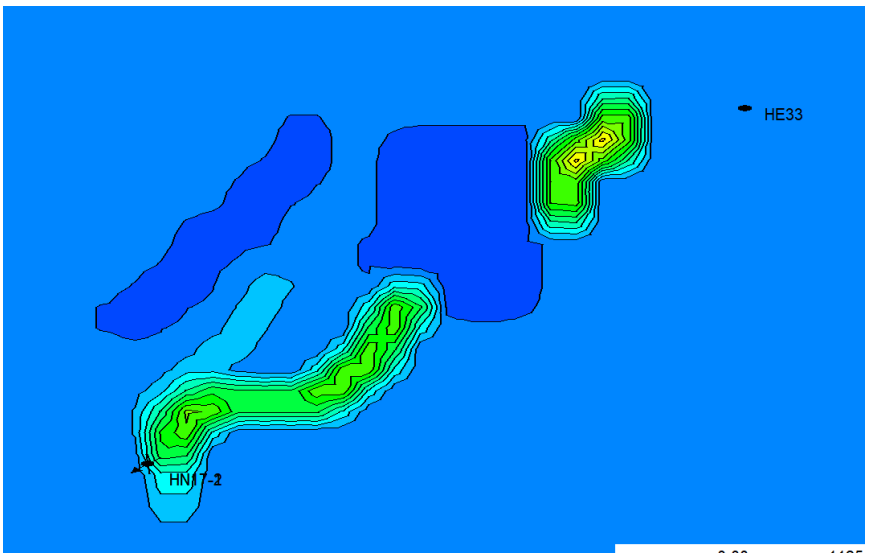

Figure 13: Areal fracture porosity distribution. The green regions represent high fracture porosity whereas, the blue regions indicate low fracture porosity.

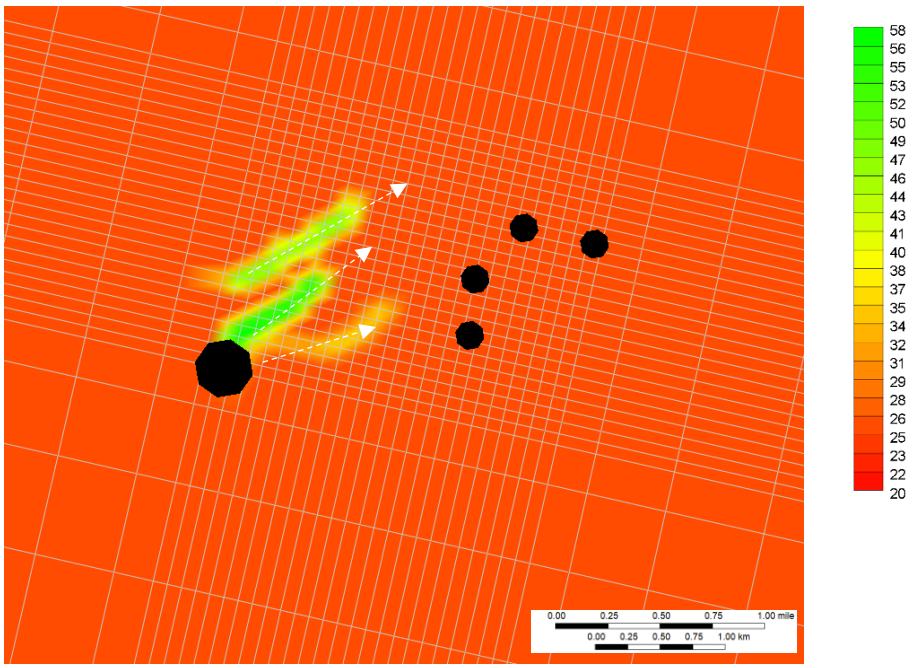

Figure 14: For the three main flow paths, multipliers for fracture permeability are illustrated as obtained from history matching. Two faults in northwest (with green colour) have higher permeability. White arrows indicate the flow paths. The black circles represent the wells. Big black circle on the left hand side is HN17 injection well, whereas pad of smaller black circles on the right hand side show the producing wells (HE31, HE48, HE44, HE33).

5. CONCLUSIONS

A series of reservoir simulations were performed to study fully coupled hydro-thermo-mechanical processes in Hellisheidi reservoir in South West Iceland during the CarbFix2 injection. The geological model was calibrated to match the tracer test using hydro-thermo-mechanical physics, where stress-dependent fracture permeability was used. The calibrated model could describe the geological model of the reservoir in terms of vertical and spatial distribution of fracture permeability and porosity. The reservoir has two high permeable layers contributing to the flow. Also, the two layers have been separated by the middle layer with relative lower permeability. In terms of porosity, the bottom section of the reservoir has lower fracture porosity compared to top layers. Fracture porosity would affect the mixing and reactions between injected and formation fluids. Furthermore, it could be identified that the northeast fault has high permeability and low porosity leading to fast flow of the injected fluid. This would affect the distribution of effective stress throughout the reservoir. In general, the model calibrated on the tracer test could be employed for further development of the reservoir for targeting the sweet spots for the fracture connectivity and heat extraction.

ACKNOWLEDGEMENT

This work is part of the Science for Clean Energy research consortium funded by European Union's Horizon 2020 research and innovation programme. For simulations, CMG software from Computer Modeling Group was used, which is appreciated.

REFERENCES

Ayala, M. A., 2010. Coupled geothermal reservoir-wellbore simulation with a case study for the Namafjall N-Iceland. Reykjavik: Faculty of Mechanical Engineering, University of Iceland.

Diehl, T., Kraft, T., Kissling, E. & Wiemer, S., 2017. The induced earthquake sequence related to the St. Gallen deep geothermal project (Switzerland): Fault reactivation and fluid interactions imaged by microseismicity. *J. Geophys. Res. Solid Earth*, Volume 122, pp. 7272-7290.

Doe, T., McLaren, R. & Dershowitz, W., 2014. Discrete Fracture Network Simulations of Enhanced Geothermal Systems. California, USA, *Thirty-Ninth Workshop on Geothermal Reservoir Engineering*.

Khodayar, M., Axelsson, G. & Steingrimsson, B., 2015. Potential Structural Flow Paths for Tracers and Source Faults of Earthquakes at Húsmúli, Hengill, South Iceland, Reykjavík: ISOR: *report ÍSOR-2015/035*.

Kristjansson, B. R. et al., 2016. Comprehensive Tracer Testing in the Hellisheiði Geothermal Field in SW-Iceland. California, USA, *41st Workshop on Geothermal Reservoir Engineering*.

Nara, Y., Meredith, P. G., Yoneda, T. & Kaneko, K., 2011. Influence of macro-fractures and micro-fractures on permeability and elastic wave velocities in basalt at elevated pressure. *Tectonophysics*, Volume 503, pp. 52-59.

Pandey, S. N., Vishal, V. & Chaudhuri, A., 2018. Geothermal reservoir modeling in a coupled thermo-hydro-mechanical-chemical approach: A review. *Earth-Science Reviews*, Volume 185, pp. 1157-1169.

Qu, Z., Zhang, W. & Guo, T., 2017. Influence of different fracture morphology on heat mining performance of enhanced geothermal systems based on COMSOL. *International Journal of Hydrogen Energy*, Volume 42, pp. 18263-18278.

Ratouis, T. M. et al., 2019. Modelling the Complex Structural Features Controlling Fluid Flow at the CarbFix2 Reinjection Site, Hellisheiði Geothermal Power Plant, SW-Iceland. California, USA, *44th Workshop on Geothermal Reservoir Engineering*.

Ruhaak, W., Heldmann, C. D., Pei, L. & Sass, I., 2017. Thermo-hydro-mechanical-chemical coupled modeling of geothermally used fractured limestone. *International Journal of Rock Mechanics and Mining Sciences*, Volume 100, pp. 40-47.

Rutqvist, J., 2015. Fractured rock stress-permeability relationships from in situ data and effects of temperature and chemical-mechanical couplings. *Geofluids*, Volume 15, pp. 48-66.

Snæbjornsdottir, S. et al., 2018. The geology and hydrology of the CarbFix2 site, SW-Iceland. *Energy Procedia*, Volume 146, pp. 146-157.

Warren, J. E. & Root, P. J., 1963. The Behavior of Naturally Fractured Reservoirs. *SPE Journal*, 3(SPE-426-PA), pp. 245-255.